Parasitology

cambridge.org/par

Toxoplasma gondii reorganizes the host cell architecture during spontaneous cyst formation *in vitro*

T. C. Paredes-Santos[1,2], E. S. Martins-Duarte[1,2], W. de Souza[1,2], M. Attias[1,2] and R. C. Vommaro[1,2]

[1]Laboratório de Ultraestrutura Celular Hertha Meyer, Universidade Federal do Rio de Janeiro – Instituto de Biofísica Carlos Chagas Filho, Rio de Janeiro, Brazil and [2]Instituto Nacional de Ciência e Tecnologia em Biologia Estrutural e Bioimagens, Rio de Janeiro, Brazil

Research Article

Cite this article: Paredes-Santos TC, Martins-Duarte ES, de Souza W, Attias M, Vommaro RC (2018). *Toxoplasma gondii* reorganizes the host cell architecture during spontaneous cyst formation *in vitro*. *Parasitology* **145**, 1027–1038. https://doi.org/10.1017/S0031182017002050

Received: 12 June 2017
Revised: 24 September 2017
Accepted: 9 October 2017
First published online: 28 November 2017

Key words:
bradyzoite; cyst formation; host–pathogen interaction; *Toxoplasma*

Author for correspondence: R. C. Vommaro, E-mail: vommaro@biof.ufrj.br

Abstract

Toxoplasma gondii is an intracellular protozoan parasite that causes toxoplasmosis, a prevalent infection related to abortion, ocular diseases and encephalitis in immuno-compromised individuals. In the untreatable (and life-long) chronic stage of toxoplasmosis, parasitophorous vacuoles (PVs, containing *T. gondii* tachyzoites) transform into tissue cysts, containing slow-dividing bradyzoite forms. While acute-stage infection with tachyzoites involves global rearrangement of the host cell cytoplasm, focused on favouring tachyzoite replication, the cytoplasmic architecture of cells infected with cysts had not been described. Here, we characterized (by fluorescence and electron microscopy) the redistribution of host cell structures around *T. gondii* cysts, using a *T. gondii* strain (EGS) with high rates of spontaneous cystogenesis *in vitro*. Microtubules and intermediate filaments (but not actin microfilaments) formed a 'cage' around the cyst, and treatment with taxol (to inhibit microtubule dynamics) favoured cystogenesis. Mitochondria, which appeared adhered to the PV membrane, were less closely associated with the cyst wall. Endoplasmic reticulum (ER) profiles were intimately associated with folds in the cyst wall membrane. However, the Golgi complex was not preferentially localized relative to the cyst, and treatment with tunicamycin or brefeldin A (to disrupt Golgi or ER function, respectively) had no significant effect on cystogenesis. Lysosomes accumulated around cysts, while early and late endosomes were more evenly distributed in the cytoplasm. The endocytosis tracer HRP (but not BSA or transferrin) reached bradyzoites after uptake by infected host cells. These results suggest that *T. gondii* cysts reorganize the host cell cytoplasm, which may fulfil specific requirements of the chronic stage of infection.

Introduction

Toxoplasma gondii is an opportunistic pathogen and the causative agent of toxoplasmosis, a disease associated with congenital neurological abnormalities, and which can be life-threatening to immunocompromised patients. Infection by *T. gondii* can also cause blindness or partial vision loss (Montoya and Liesenfeld, 2004).

Toxoplasma gondii is able to infect all nucleated cells from warm-blooded animals, and the parasite is adapted to intracellular life. In the acute stage of infection, parasites actively invade host cells and establish a PV, where the tachyzoite forms replicate by endodiogeny (Sheffield and Melton, 1968; Dubey *et al.* 1998). After several rounds of replication, tachyzoites egress from host cells, causing cell lysis, and restart the lytic cycle in neighbouring cells (Blader *et al.* 2015), causing tissue destruction and disease pathology. In the acute stage of infection, an interferon-γ-mediated immune response triggers the conversion of tachyzoites into bradyzoites, the slow-diving, chronic disease forms that reside in modified PVs called tissue cysts (Suzuki *et al.* 1988; Sullivan and Jeffers, 2012). These resistant modified PVs preferably locate in cells from the central nervous system and skeletal muscle cells, 'immune-shielded' tissues where bradyzoites remain hidden and protected from destruction by immune response mechanisms, during chronic infection (Weiss and Kim, 2000).

The process of tachyzoite to bradyzoite conversion (also referred to as cystogenesis) is a remarkable event in *T. gondii* biology, and allows parasite persistence throughout the lifespan of intermediate hosts, as well as 'silent' parasite transmission between intermediate hosts (Sullivan and Jeffers, 2012). The cyst is delimited by a cyst wall that represents a remnant of the parasitophorous vacuole membrane (PVM), which becomes convoluted and thicker because of the highly glycosylated proteins that accumulate in the internal face of the PVM (Ferguson and Hutchison, 1987; Zhang *et al.* 2001; Lemgruber *et al.* 2011; Tomita *et al.* 2013).

Toxoplasma gondii is auxotrophic for several nutrients, including cholesterol, purines and tryptophan, which must be obtained from the host cell (Coppens, 2014).While the PV provides a perfect environment for parasite proliferation and avoidance of host immune responses, it is also a barrier for nutrient harvesting by the parasite. Tachyzoites are able to ingest and digest host-derived proteins (Dou *et al.* 2014), and the PVM is permeable to

CAMBRIDGE UNIVERSITY PRESS

molecules of up to 1·9 kDa (Schwab *et al.* 1994; de Souza and Attias, 2015). The dense granule proteins GRA 17 and GRA 23 are secreted by the tachyzoites and mediate the exchange of small molecules between *T. gondii* and the host cell cytoplasm, forming pores in the PVM (Gold *et al.* 2015). Also, tachyzoite infection is characterized by clear host cell organelle repositioning aimed at diverting host cell nutrients to the PV (Romano and Coppens, 2013).

As soon as the tachyzoite invades a host cell, the non-fusogenic PV migrates to the perinuclear region (Wang *et al.* 2010), and the centrosomes are pulled to the vicinity of the PV (Walker *et al.* 2008), leading to a global reorganization/recruitment of host cell structures (including microtubules, mitochondria, the endoplasmic reticulum, the Golgi complex and lysosomes) around the PV (Sinai *et al.* 1997; Magno *et al.* 2005; Coppens *et al.* 2006; Pernas *et al.* 2014). Later, mitochondrial profiles and ER tubules can be seen around the PV, and in close contact with the PVM, although the association of mitochondria with the PVM is dependent on the parasite strain (Pernas *et al.* 2014). Importantly, tachyzoites divert host cell lysosomal content (LDL) to the PV by vesicular transport dependent on host microtubules, which are inserted into the PV and governed by the secreted *Toxoplasma* protein GRA7 (Coppens *et al.* 2006). Furthermore, the parasite scavenges sphingolipids from the host Golgi complex, by sequestering Golgi-derived Rab vesicles (Romano *et al.* 2013).

Comparatively less is known about the interaction of *T. gondii* cysts with the host cell cytoplasm, and the host cell architecture during and after cyst formation has not been studied in detail. While a proportion of parasites within cysts remain in the G0 stage (White *et al.* 2014), the cyst grows with time, because some cysts continue to divide at a slow rate (Watts *et al.* 2015). Also, bradyzoites can spread the infection to neighbouring cells *in vitro* (Dzierszinski *et al.* 2004), without total cell wall rupture (Dzierszinski *et al.* 2004). These data indicate that cysts are metabolically active, and are likely to scavenge nutrients from the host cell. However, survival within the strengthened cyst wall, which guarantees long-term infection persistency (Ferguson and Hutchison, 1987), also represents a considerable barrier to the diversion of host resources to the cyst. During cyst infection, our group showed that cysts possess a size-selective permeability to molecules of up to 10 kDa (Lemgruber *et al.* 2011). Also, cationic markers adhere to the cyst wall membrane are able to reach the cyst lumen (Guimarães *et al.* 2007).

Given that cysts appear to be metabolically active and are capable of molecular interchange with the host cell cytoplasm, we hypothesized that the scavenging of host molecules continues during cyst formation, and in chronic infection. To examine this hypothesis, we studied the positioning of host cell structures/organelles in chronically infected cells *in vitro*, using the EGS strain. Previously, we described that this *T. gondii* hybrid strain has a high ratio of spontaneous cystogenesis in cell culture (Paredes-Santos *et al.* 2013), representing a valuable tool to study different aspects of the gradual conversion of PVs (containing tachyzoites) into cysts (containing bradyzoites) *in vitro*, while avoiding the artefacts of stress-induced cystogenesis protocols (Paredes-Santos *et al.* 2013, 2016).

We present here a detailed view of organelle repositioning in cells with cysts, by combining a variety of light and electron microscopy techniques, including immunofluorescence, live cell imaging, super-resolution structured illumination (SR-SIM) imaging and electron microscopy (conventional thin-sections and tomography). In addition, we used endocytosis assays to visualize nutrient uptake by cysts in the intracellular environment. Our data show that *T. gondii* cyst formation and intracellular maintenance involve specific changes in the cytoplasmic organization of infected host cells. These changes are likely to fulfil specific requirements for nutrient uptake mechanisms in the chronic stage of infection, which may be different from those in the acute (tachyzoite-based) stage.

Methodology

Ethics statement

This study was approved by the Ethics Committee for Animal Experimentation of the Health Sciences Centre, Federal University of Rio de Janeiro (Protocol numbers IBCCF 099/100). All animals received humane care in compliance with the 'Principles of Laboratory Animal Care' formulated by the National Society for Medical Research (USA) and the 'Guide for the Care and Use of Laboratory Animals', prepared by the National Academy of Sciences (USA).

Host cells

LLC-MK_2 cells (ATCC© # CCL-7) (epithelial kidney cells from *Macaca mullata*) and human foreskin fibroblasts (HFF; ATCC© # SCRC-1041™) were used in infection assays. Cells were maintained in RPMI (LLC-MK_2) and DEMEM High Glucose (HFF) media (both from Invitrogen) supplemented with 2 mM L-glutamin, 10% FBS and 2 mg mL^{-1} penicillin/streptomycin (Invitrogen).

Maintenance of cyst reservoirs in vivo

The following *Toxoplasma gondii* strains were used in this study: wild-type EGS (Vieira *et al.* 2002; Ferreira *et al.* 2006) and Bag1-EGFP (Bgreen strain; also in the EGS background) (Paredes-Santos *et al.* 2016). To preserve the ability for high-rate spontaneous cyst formation, typical of the EGS strain, bradyzoites were maintained as a cyst reservoir in infected mice, and every 60 days a fresh batch of bradyzoites, isolated from infected brain tissue, was used to infect LLC-MK_2 cells. The parasites used in all spontaneous cystogenesis experiments were obtained from the supernatant of routinely infected LLC-MK_2 cultures (see the section 'Parasite maintenance *in vitro*').

The cyst reservoir was maintained by serial passages in chronically infected Swiss mice. Cysts obtained from the brain of previously infected animals were administered to uninfected animals by oral gavage (50 cysts/animal). The symptoms/effects of the acute phase of infection by EGS were controlled by treating infected animals with 0·5 mg mL^{-1} of sulfadiazine (Sigma-Aldrich, St. Louis, USA) in the drinking water, from 48 h post infection, and for the following 10 days. Chronically infected animals were maintained for 50 days, and then humanely euthanized, after which infected brains were collected for bradyzoites isolation from tissue cysts, as described below. A total of 15 animals were used in this study.

Bradyzoite isolation from mouse brain tissue cysts

The isolation of cysts from infected brains was performed as described previously (Freyre, 1995). Briefly, brains were homogenized in Hanks solution (Sigma-Aldrich, St. Louis, USA) by repeated passage through 18–25 Gauge needles. Afterwards, samples were centrifuged at 400 ***g*** for 10 min, the pellet was resuspended in 25% (w/v) Dextran 150 000 kDa (Sigma-Aldrich, St. Louis, USA) in Hanks, and samples were centrifuged at 2200 ***g*** for 10 min. The final pellet, containing cysts, was washed 3 times in phosphate buffered saline (PBS), to remove the dextran and then resuspended in RPMI and were used immediately for bradyzoite isolation.

https://doi.org/10.1017/S0031182017002050 Published online by Cambridge University Press

To obtain viable bradyzoites from isolated tissue cysts (Popiel *et al.* 1996), the cyst wall was digested by adding pepsin digestive fluid (0·01% pepsin, 1% NaCl and 0·28% HCl in distilled water) diluted to 1:5 in PBS, and the suspension was incubated for 2 min at 37 °C. Digestion was stopped by placing tubes on ice and adding 1% sodium carbonate in water, followed by dilution in RPMI medium and centrifugation at 2200 ***g*** for 10 min. The pellet, containing viable bradyzoites, was resuspended in RPMI and used for infection of LLC-MK_2.

Parasite maintenance in vitro

Bradyzoites isolated from brain tissue cysts as described above were used to infect confluent monolayers of LLC-MK_2 cells (at a ratio of 10:1 parasites per cell). Infected LLC-MK_2 cultures were passaged by trypsinization, and kept for a maximum of 60 days. To avoid monolayer disruption by the presence of free tachyzoites, the medium was changed every 48 h and free tachyzoites were removed. The parasite population found in the supernatant of infected LLC-MK_2 cultures – which typically consists of ~97% tachyzoites and ~3% bradyzoites (Paredes-Santos *et al.* 2013) – was used in all spontaneous cystogenesis experiments.

Spontaneous cystogenesis

For spontaneous cyst formation *in vitro*, parasites collected from the supernatant of previously infected LLC-MK_2 monolayers were used to infect LLC-MK_2 or HFF cells (at 90% confluency), at a multiplicity of infection of 5:1. LLC-MK_2 or HFF host cells were chosen for each assay depending on specific technical requirements (such as the availability of species-specific antibodies). Infected cells were kept for 96 h at 37 °C (with 5% CO_2), to establish the bradyzoite infection, and then processed for transmission electron microscopy (TEM) or immunofluorescence assays (IFA), as described below.

Drug treatments

Drug treatments on infected cells subjected to spontaneous cystogenesis were initiated 24 h post-infection, to avoid detrimental effects of drugs on invasion or infection establishment. Treatments lasted for 72 h (completing the 96 h chronic infection period), and samples were then examined by IFA (as described below). The following drug treatments were used in this study: 100 nM Paclitaxel-taxol (Sigma-Aldrich, St. Louis, USA) 2 $\mu g\ mL^{-1}$ tunicamincin-A (Sigma-Aldrich, St. Louis, USA), and 2·5 μM brefeldin-A (Sigma-Aldrich, St. Louis, USA) at. Controls with vehicle DMSO were performed. The MTS assay (AbCam) was used to determine the optimal drug concentrations that had minimal effect on cell viability, for the duration of the assays (not shown).

Immunofluorescence assays

Chronically infected cells adhered to Labtek™ (Thermo Fisher) slides were fixed for 20 min at room temperature with 4% formaldehyde (freshly prepared) diluted in PBS (2). Then samples were permeabilized with 0·5% Triton X-100 (in PBS) for 20 min; alternatively, samples were permeabilized with 0·02% Saponin (Sigma) (w/v), diluted in 'blocking buffer', for the localization of endolysosomal vesicles (i.e. for probing with anti-EEA1 and anti-Rab7, anti-Rab11, anti-LAMP1). After permeabilization, all samples were incubated in 'blocking buffer' (PBS, pH 7·3, containing 1·5% bovine serum albumin and 0·5% of cold water fish gelatin, both from Sigma) for 1 h at room temperature.

Then, samples were incubated, for 1 h, at room temperature, with the following probes (alone or in combination, and diluted in blocking buffer): anti-CST-1 mAb (kindly provided by Dr Louis M. Weiss) or 0·01 $mg\ mL^{-1}$ *Dolichos biflorus agglutin* (DBA) conjugated with FITC or TRITC (VectorLab), to detect the cyst wall; phalloidin-Alexa 546 (Invitrogen, cat no A22283; used according to the manufacturer's recommendations); anti-α−tubulin mAb (Sigma, cat no T5168; dilution 1:200), anti-vimentin pAb (Cell Signalling, cat no D21H3, dilution 1:100), anti-PDI pAb (Sigma, cat noP7372; dilution 1:100), anti-COX IV pAb (Cell Signalling, cat no 3E11; dilution 1:100), anti-RCSA1 pAb (Cell Signalling, cat no D2B6N; dilution 1:100), anti-EEA1 pAb (Cell Signalling, cat no2411S; dilution 1:100), anti-Rab7 pAb (Cell Signalling, cat no D95F2; dilution 1:100), anti-Rab11 pAb (Cell Signalling, cat no D4F5; dilution 1:100), anti-LAMP1 pAb (Cell Signalling, cat no D2D11; dilution 1:100).

Samples were incubated with secondary antibodies conjugated with Alexa 488, 546 or 633 (Molecular Probes), at a 1:500 dilution. Controls were performed by omitting the primary labelling step. Then, coverslips were incubated with 0·5 $\mu g\ mL^{-1}$ Hoechst 33342 (ThermoFisher, Cat. no. H1399) for 10 min. Coverslips were then mounted onto slides using Prolong Gold Antifade (Invitrogen). Samples were imaged in a Leica DMI 6000 epifluorescence microscope, and in a Leica SP3 laser scanning confocal microscope.

Endocytosis assays

Chronically infected cells (see the section 'Spontaneous cystogenesis') and uninfected monolayers were subjected to fasting for 30 min (at 37 °C, in RPMI medium without FBS), and then incubated (for up to 1 h, at 37 °C and 5% CO_2) in the same medium containing one of the following endocytic tracers (diluted to 1:10): Transferrin conjugated to 10-nm gold (Tf-Au) or horseradish peroxidase (HRP-Sigma) was used as fluid-phase tracer at a final concentration of 1 $mg\ mL^{-1}$ in culture medium, for electron microscopy imaging; and transferrin-Alexa 994 (Invitrogen®) or Albumin-Alexa 594, for detection by fluorescence microscopy. After the incubation with tracers, cells were fixed and processed for TEM (as described below) or imaged by fluorescence microscopy (as described in the section 'Immunofluorescence assays').

3-3′-diaminobenzidine (DAB) cytochemistry

For DAB cytochemistry, cells that had taken up HRP as described above were incubated in a solution containing 0·5 $mg\ mL^{-1}$ DAB (Sigma) in Tris-HCl buffer, pH7·6, for 15 min (in the dark, and at RT). Then, H_2O_2 was added to a final concentration of 0·03% (v/v), and samples were incubated for a further 15 min in the same conditions. After that, samples were washed in the same buffer and processed for TEM or optical microscopy, as described in other section (see the sections Transmission electron microscopy and Endocytosis assays sections).

Live cell imaging

Chronically infected cells (see the section 'Spontaneous cystogenesis') on 35-mm Matek dishes were incubated for 1 h at 37 °C with Lysotracker RED (ThermoFisher), washed with PBS and then imaged for a total of 3 h (at 5-min intervals) in a Zeiss Axio observer microscope (at 37 °C and 5% CO_2). The Image J software was used for image analysis.

Super-resolution structured illumination microscopy

Samples prepared for immunofluorescence as described above were subjected to SR-SIM in an ELYRA S.1 microscope (Carl Zeiss Microimaging), equipped with a 488-nm laser (100 mW),

https://doi.org/10.1017/S0031182017002050 Published online by Cambridge University Press

a 61-nm laser (100 mW) and an Andor EM-CCD camera (iXon DU 885). Thin (0·1 mm) Z-stacks of high-resolution image frames were collected in 5 rotations by utilizing an alpha Plan-Apochromat 63×/1·46 oil DIC M27ELYRA objective. Images were reconstructed using a structured illumination algorithm in the ZEN software (blackedition, 2011, version 7.04.287).

Transmission electron microscopy

LLC-MK_2 monolayers infected as described above (see the section 'Spontaneous cystogenesis') were processed for TEM *in situ* (i.e. in the culture flasks), as described previously (Magno *et al.* 2005), to maintain the orientation/arrangement of the cells and cysts. Briefly, samples were washed with PBS, fixed overnight (at 4 °C) with 2·5% glutaraldehyde in 0·1 M cacodylate buffer (pH 7·2), rinsed in the fixation buffer and post-fixed in 1% osmium tetroxide and 1·25% of potassium ferrocyanide in 0·1 M sodium cacodylate buffer (pH 7·2). Then, samples were dehydrated in series of ethanol solutions from 50% to 100% (for 10 min in each step), and embedded in Embed 812 (Electron Microscope Science) resin. Ultrathin sections were cut *en face* and stained with 5% uranyl acetate and lead citrate, then observed in a Zeiss EM900 transmission electron microscope.

The number of mitochondrial profiles associated (i.e. mitochondrial profiles attached to the PVM or cyst membrane) with the membrane of the PV or cyst was quantified from 15 000×-magnification TEM images of a total of 77 LLC-MK_2 cells with both cysts and PVs, from 3 independent experiments. We calculated the percentage of PV or cysts with mitochondria-associated and the number of profiles associated with each PV or cyst.

Electron microscopy tomography (ET)

For ET, semi-thin sections (200–250 nm) of samples embedded for TEM as described above were subjected to the second round of post-sectioning contrast with uranyl acetate and lead citrate, and imaged without fiducial markers. Images were taken at 200 kV, in a Tecnai 20 LaB6-FEI transmission electron microscope equipped with a CCD Temcam F214 camera (TVIPS GmbH), with an increment of 1° between images, and a tilt range from −60 to +60 for single axis tomography. Sections were pre-irradiated (for 2 min) to avoid shrinking effects during recording. Automated data acquisition of the tilt series was carried out using Xplore 3D (FEI Company). Tomograms were computed for each tilt axis using the R-weighted back-projection algorithm and combined into one double-tilt tomogram using eTomo (Kremer *et al.* 1995).

The proximity between mitochondria (outer membrane) and the membrane of the PV or cyst was measured using 3 different ET samples of cells infected with PVs and cysts (both mature and immature). The software IMOD was used to determine the shortest distances between membranes, in 3D volumes of tomograms from 200-nm sections.

Results

Host cell microtubules and intermediate filaments (but not microfilaments) form a 'cage' around cysts

The intracellular survival of *T. gondii* tachyzoites involves the diversion of cellular resources to the PV, associated with the global restructuring of the host cell architecture (Romano and Coppens, 2013). In contrast, the architecture of host cells infected with *T. gondii* bradyzoites has not been described, although bradyzoites (the chronic infection forms found within cysts) appear to be metabolically active (Watts *et al.* 2015), and cysts are likely to mobilize cellular resources to maintain chronic infection.

To analyse the organization of cytoplasmic components around *T. gondii* cysts, we infected LLC-MK_2 and HFF cells with *T. gondii* tachyzoites and analysed infected cells 96 h post-infection (henceforth referred to as 'bradyzoite' infection), when cyst formation is observed in ∼40% of cells infected with the EGS strain (Paredes-Santos *et al.* 2013). Due to the spontaneity of the PV-to-cyst conversion in the EGS strain, bradyzoite infected monolayers had mixed infection with PVs and cysts (typically at 40 and 60% per cell, respectively; Paredes-Santos *et al.* 2013), allowing the comparison between acute (PV-associated) and *in vitro* chronic stage (cyst-associated) local cytoplasmic reorganization, within the same cell. As well as the wild-type EGS strain, we also used EGS parasites stably expressing the bradyzoite antigen BAG-1 tagged with GFP (Bgreen strain; Paredes-Santos *et al.* 2016), to allow cysts, containing green bradyzoites, to be clearly distinguished from PVs, containing tachyzoites.

Initially, we analysed the cytoskeletal modifications associated with bradyzoite infection, by labelling three types of cytoskeletal components in bradyzoite infected cells: actin microfilaments (labelled with phalloidin), microtubules (labelled with an anti-α-tubulin antibody) and intermediate filaments (labelled with an anti-vimentin antibody) (Fig. 1). In these cells, cysts were detected by staining of the cyst wall glycosylated proteins with the lectin DBA.

The host cell microfilaments did not reach/surround the cyst boundary in chronically infected cells (Fig. 1A and B). The chronic infection did not disrupt the organization of host cell microfilaments, or stress fibre formation, in HFF cells (Fig. 1A). Similarly, the cortical pattern of actin filaments did not change during cyst formation in infected LLC-MK_2 cells (Fig. 1B).

In contrast, the intermediate filament network was reorganized around the cysts (arrows) and PVs (arrowhead) in infected HFF labelled for vimentin (Fig. 1D). Also, SR-SIM analysis confirmed that vimentin filaments were associated with cyst wall elements (Fig. 1E). In TEM images of infected cells, bundles of intermediate filaments surrounded the cyst wall (Fig. 1F). Our results were similar to previously reported data showing the recruitment of the intermediate filament network to the site of infection, both in the chronic and in the acute stage of infection (Halonen and Weidner, 1994; Halonen *et al.* 1998).

Aside from the intermediate filament network, the distribution of microtubules in host cells also changed dramatically upon cyst formation (Fig. 1G and H), similar to that observed previously for acute (tachyzoite) infection (Andrade *et al.* 2001; Melo *et al.* 2001; Coppens *et al.* 2006; Sweeney *et al.* 2010). In chronically infected LLC-MK_2 and HFF cells, the cage of microtubules typically observed surrounding the nucleus was seen surrounding the cysts instead (Fig. 1G and H). Also, imaging of infected cells by SR-SIM revealed that the microtubules were closely associated with the cyst wall (Fig. 1H), and TEM analysis showed that cysts were surrounded by a microtubule cage (Fig. 1I).

The importance of microtubule dynamics for *T. gondii* tissue cyst development was analysed by quantifying cyst formation 96 h post-infection, in HFF cells that were treated with the microtubule stabilizer taxol for 72 h (from 24 h post-infection). Taxol treatment did not disrupt the cage of microtubules found around PVs and cysts (data not shown), and the number of cysts increased by 50% in taxol-treated cells, compared with the untreated (Fig. 1C), suggesting that the stabilization of a microtubule cage around the PV favours bradyzoite development and cyst formation.

Altogether, these results show that host cell microtubules and intermediate filaments (but not the actin cytoskeleton) were reorganized under bradyzoite infection in cells containing cysts of *Toxoplasma*, in comparison with non-infected cells.

https://doi.org/10.1017/S0031182017002050 Published online by Cambridge University Press

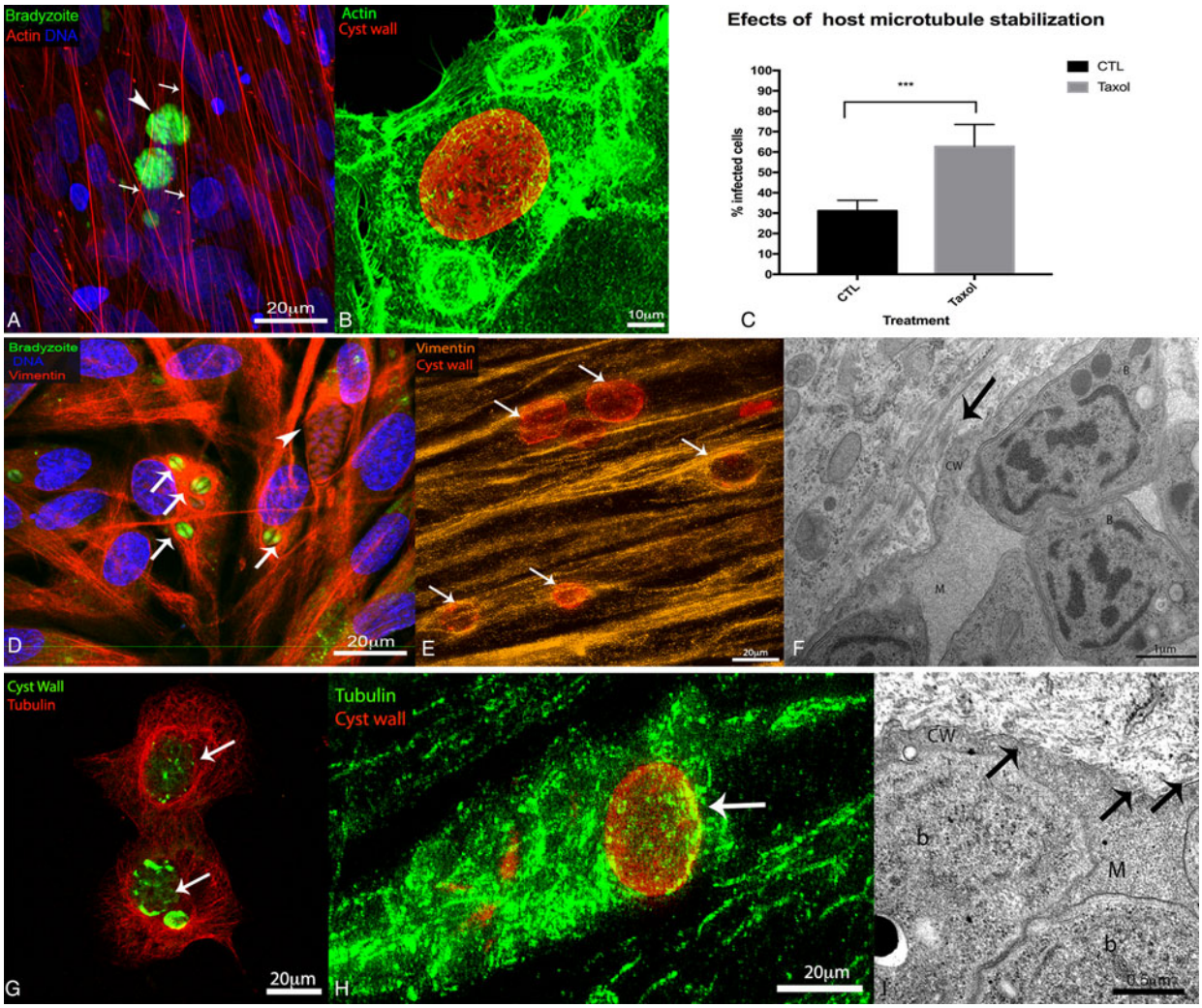

Fig. 1. Cytoskeletal organization of host cells infected with *Toxoplasma gondii* cysts. LLC-MK2 and human foreskin fibroblasts (HFF) cells were subjected to chronic infection with wild-type EGS or with the Bgreen strain (which produces GFP-labelled bradyzoites) and then labelled for markers of different cytoskeletal elements (for observation by fluorescence microscopy; A, B, D, E, G, H), or processed for transmission electron microscopy (TEM; F–I). For fluorescence microscopy, wild-type cysts were identified by labelling of the cyst wall with *Dolichos biflorus agglutin* (DBA)-FITC, and the DNA was labelled with Hoescht 33342. (A, B) Distribution of microfilaments in HFF (A) and LLC-MK_2 (B) labelled with phalloidin (in red or green, in A and B, respectively). (A) The organization of fibroblast stress fibres (arrows) observed in bradyzoites (arrowhead) infected cells. Scale bar: 20 μm. (B) Cortical actin distribution in infected cells containing *Toxoplasma* cysts (red). Scale bar: 10 μm. (C) Effect of treatment of infected HFF with 100 nM taxol for 72 h (starting from 24 h post-infection). The percentage of cells with cysts or PVs was quantified after 96 h of infection. Data represent median ± S.D. values of three independent experiments ($P < 0{\cdot}005$) (by one-way analysis of variation (ANOVA)). (D) Distribution of intermediate filaments in HFF infected with Bgreen parasites. Intermediate filaments (labelled with an anti-vimentin antibody, in red) accumulate around the cysts (arrows), which contain bradyzoites (in green), but not around parasitophorous vacuoles (PVs) (arrowheads). Scale bar: 20 μm. (E) Super resolution-structured illumination microscopy (SR-SIM) of HFF infected with cysts (in red) and labelled with an anti-vimentin antibody (orange), showing co-localization of intermediate filaments with the cyst wall (arrows). Scale bar: 20 μm. (F) TEM image of host cells showing intermediate filaments (arrow) surrounding the cyst wall. Scale bar: 1 μm. (G) Distribution of microtubules (in red, labelled with an anti-tubulin antibody) in LLC-MK_2 cells, where microtubules appear to surround the cysts (in green; arrows). Scale bar: 20 μm. (H) SR-SIM of HFF infected with cysts (in red) and labelled with an anti-alpha tubulin antibody (green), showing co-localization of intermediate filaments and microtubules with the cyst wall (arrows). Scale bar: 20 μm. (I) TEM images of host cells showing microtubules (arrows) surrounding the cyst wall. In F and I: b – bradyzoite, m – cyst matrix, cw – cyst wall. Scale bar: 0·5 μm.

ER lamellae accumulate around the cyst and are interdigitated with cyst wall folds

The reorganization of microtubules around the cyst wall is expected to allow the recruitment of organelles towards the cyst. Thus, we sought to visualize the distribution of secretory organelles in chronically infected cells using markers for the Golgi complex lamellae (the receptor binding cancer antigen expressed on SiSo cells, or RCSA-1), and the endoplasmic reticulum cisternae (protein disulphide isomerase, or PDI).

In infected HFF, the Golgi complex appeared either near the cyst, on the nuclear periphery (Fig. 2A), or on the opposite side of the nucleus to where the cysts were located (Fig. 2B). The 3D volume reconstruction of a cyst boundary by electron tomography showed that the Golgi was often near the cyst, but did not appear associated with the cyst membrane (Supplementary Fig. S1). Thus, we did not observe an association between the Golgi and the cyst, since the relocation of this organelle was not mandatory during chronic infection, while the Golgi complex reallocates around tachyzoite PVs (Romano *et al.* 2013).

In contrast, endoplasmic reticulum (ER) profiles were always observed around the cyst wall boundary. When observed by TEM, 100% of cysts formed *in vitro* had membrane profiles associated with ER lamellae. Images obtained by SR-SIM and TEM showed that ER profiles were intimately associated with the cyst wall (Fig. 2D–E). This association is evident in 3D volume images produced by electron microscopy tomography, where ER profiles were juxtaposed to the membrane of the immature cyst (Fig. 2E), and projected into folds in the cyst wall membrane of mature cysts (Fig. 2E, Supplementary Fig. S1); however, fusion between ER and cyst

https://doi.org/10.1017/S0031182017002050 Published online by Cambridge University Press

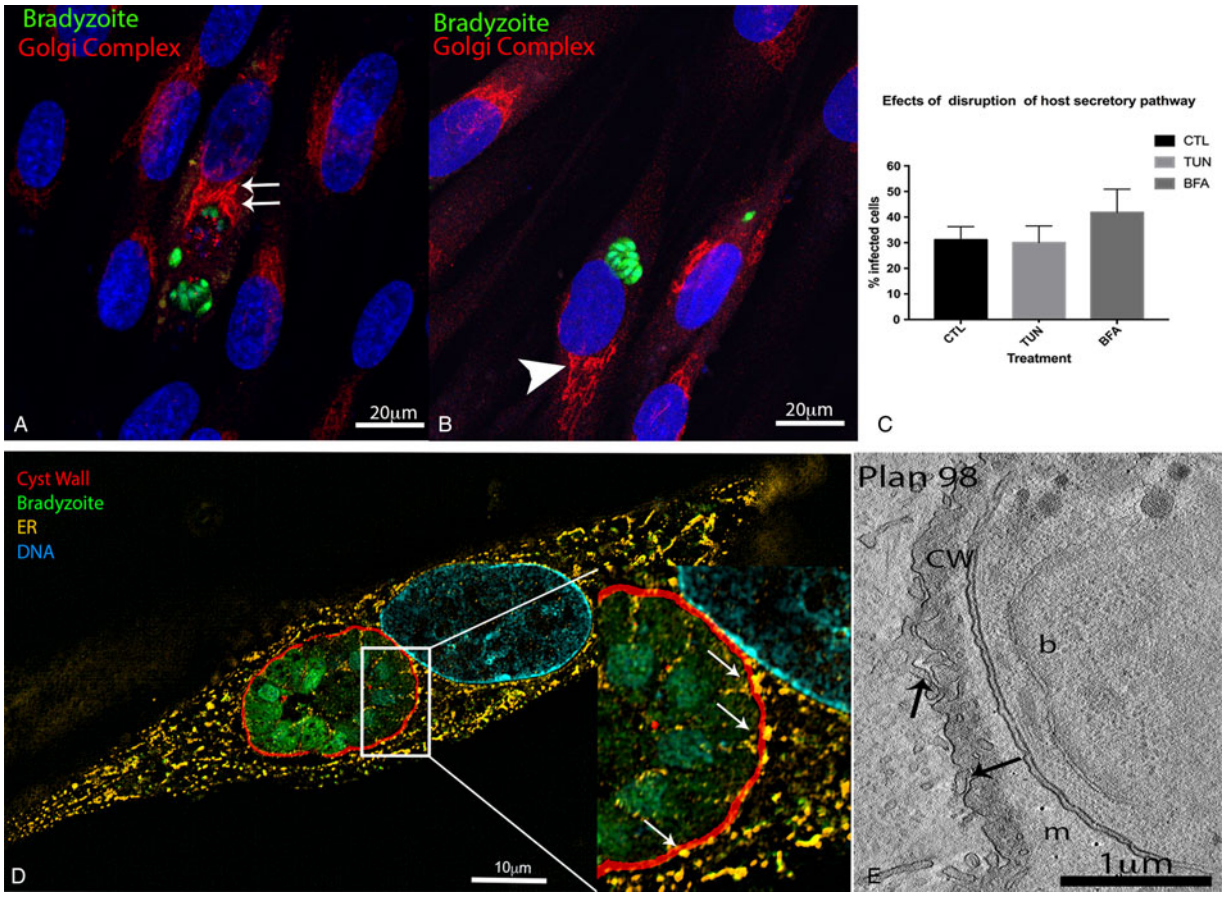

Fig. 2. Localization of secretory organelles in cells infected with *Toxoplasma gondii* cysts. The localization and role of secretory organelles (Golgi complex and endoplasmic reticulum (ER)) during *T. gondii* cyst formation was evaluated in human foreskin fibroblasts (HFF) subjected to chronic infection with the Bgreen strain (which produces GFP-labelled bradyzoites). For fluorescence microscopy, the DNA was labelled with Hoescht 33342, and the following antibodies were used to recognize parasite and host cell structures: anti-RCSA-1 (Golgi stacks), anti-PDI-1 (ER lamellae) and anti-CST-1 (cyst wall). (A, B) Immunofluorescence images showing the localization of Golgi stacks in cells infected with cysts (bradyzoites expressing GFP). In some cells, the Golgi stacks were on the opposite side of the cell to where the cyst was found (arrowhead in A), while in others the stacks were next to the cyst (double arrows in B). Scale bars: 20 μm. (C) Effect of treatment of chronically infected HFFs with 2·5 μM of brefeldin A (BFA) or 2 μg mL^{-1} of tunicamicin (TUN) for 72 h (starting from 24 h post-infection). The percentage of cells with cysts or parasitophorous vacuoles (PVs) was quantified 96 h post-infection. Data represent median ± S.D. values of two independent experiments. The differences between treated and untreated (control, CTL) groups were not statistically significant (by one-way ANOVA). (D) Super resolution-structured illumination microscopy (SR-SIM) of HFF infected with cysts (with bradyzoites in green, and the cyst wall in red), showing co-localization of ER lamellae with the cyst wall (arrows in the zoomed area). Scale bars: 10 μm. (E) Electron microscopy tomography slice of an infected cell showing ER profiles juxtaposed to an immature cyst wall (arrows). Scale bars: 1 μm.

membranes was never observed. Altogether, these data demonstrate that ER elements are intimately associated with the cyst wall membrane.

To evaluate the importance of the association between toxoplasma cysts and the Golgi complex and the ER, we treated infected HFF for 72 h (starting at 24 h post-infection) with tunicamycin or brefeldin A, which disrupt essential functions of the ER and Golgi. Tunicamycin impairs the N-glycosylation of proteins, and brefeldin A disrupts the anterograde traffic between the ER and the Golgi complex. Infected cells were treated with drugs and cyst formation was quantified 96 h post-infection. Treatment with tunicamycin or brefeldin A had no statistically significant effect on cyst formation in HFF cells (Fig. 2C). It is important to note that treatment with 2 μg mL^{-1} tunicamycin for 72 h did not affect host cell viability, as measured using the MTS assay (data not shown).

Mitochondria appeared adhered to the PV membrane, but not to the cyst wall

The reorganization of microtubules around the cyst led to the recruitment of mitochondria (Fig. 1G and H), whose distribution in the cytoplasm is microtubule-dependent (Bereiter-Hahn and Vöth, 1994). Immunofluorescence microscopy for the mitochondrial marker COX-IV showed that mitochondria concentrated around both PVs (containing tachyzoites; Fig. 3B) and cysts (containing bradyzoites; Fig. 3C), in infected HFF, while uninfected cells had sparsely distributed mitochondria (Fig. 3A).

However, in TEM sections of infected LLC-MK$_2$ cells, we observed a clear difference between cysts and PVs regarding their association with mitochondria (Fig. 3D–J). Mitochondria often appeared attached to the PV membrane, with long sections of the mitochondrial membrane juxtaposed to the PV membrane (Fig 3G). In contrast, mitochondria were observed close to the cyst, but did not appear adhered to the cyst wall (Fig. 3G, I and J). We quantified the association of mitochondria with PVs and cysts in TEM ultrathin-sections of chronically infected cells (77 images at 15 000 × magnification, pooled together from 3 independent experiments; Fig. 3D–F). We found that only 39% of cysts had closely associated mitochondrial profiles, while mitochondrial profiles were found associated with 97% of PVs (Fig. 3D). The number of closely-associated mitochondrial profiles also varied between cysts and PVs (Fig. 3F); on average, 3 mitochondrial profiles were associated with PVs, *vs.* an average of 1 associated with cysts. On average, 19% of the PVM perimeter had an associated mitochondrial profile (Fig. 3E). These data show a clear difference in the association of mitochondria with

https://doi.org/10.1017/S0031182017002050 Published online by Cambridge University Press

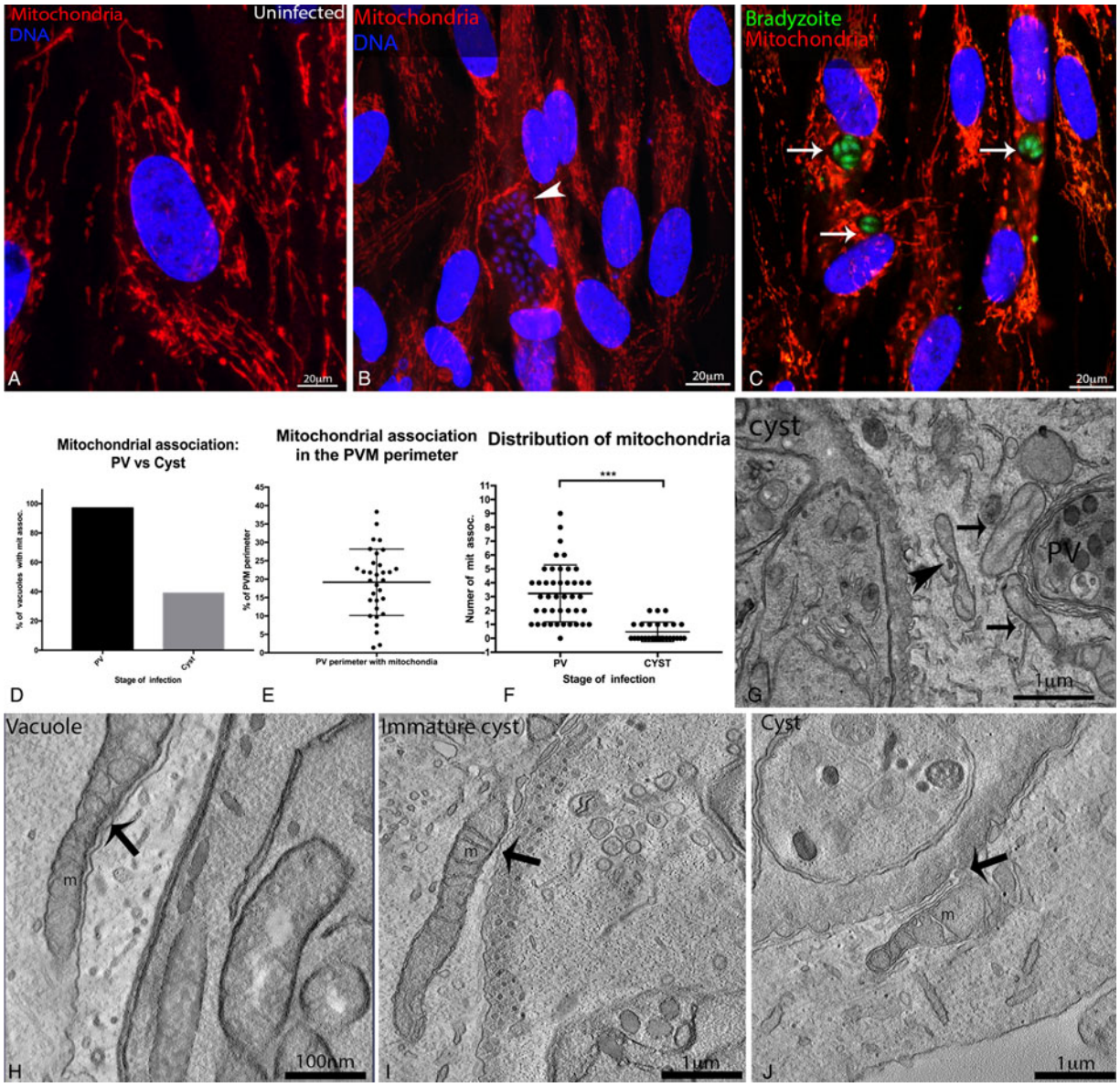

Fig. 3. Localization of mitochondria in cells infected with *Toxoplasma gondii* cysts. human foreskin fibroblasts (HFF) were subjected to chronic infection with the Bgreen strain (which produces GFP-labelled bradyzoites) and the distribution of mitochondria was evaluated by fluorescence (A–C) and electron (F–I) microscopy. For fluorescence microscopy, mitochondria were labelled with an anti-COX 4 antibody (in red) and the DNA was labelled with Hoescht 33342, the cyst wall was stained with anti-CST1. Mitochondrial distribution in uninfected HFF (A), and in cells infected with parasitophorous vacuoles (PVs, arrowhead in B) or with cysts (identified by the presence of green bradyzoites; arrows in (C). Scale bars: 20 μm. (D) Percentage of PV and cysts with associated mitochondrial profiles (data represent the quantification from pooled images from 3 independent experiments) the number of PV containing mitochondrial association is 3-fold higher then cysts. (E) Percentage of the PV perimeter associated with mitochondrial profiles (19% on average, varying from 1 to 38%, in 43 TEM). (F). Distribution of mitochondrial association between intracellular cysts and PVs. The average number of mitochondrial profiles associated with PVs was 3 fold higher than for cysts (*T*-test, $P < 0{\cdot}0001$). (G) Transmission electron microscopy (TEM) images of cells infected simultaneously with PVs and cysts, showing mitochondria closely associated with the PV membrane (arrows), but somewhat distant from the cyst wall membrane (arrowhead) Scale bars: 1 μm. (H–J) Electron microscopy tomography slices of infected cells showing mitochondrial profiles (m) tightly associated with the PV membrane (H), but less closely associated with the immature cyst membrane (I) or the mature cyst wall (J) (arrows). Scale bars: 100 nm.

cysts and PVs, showing that the PV has the ability to recruit more mitochondria to its vicinity than the cyst.

In addition, the distance between the membrane of the cyst wall and the external membrane of the mitochondria was measured in three different stages of cyst formation, in ~200-nm thick electron microscopy tomograms. During tachyzoite infection, the shortest distance measured between the mitochondria and the PV membrane was 9·7 nm (Fig. 3H). This value is very similar to the distance of 10·1 nm observed for specific points of contact between mitochondria and the membrane of immature cysts, identified as modified PVs with a thick – but not completely formed – cyst wall and a developing intracystic network (Fig. 3I). However, mitochondria did not appear adhered to immature cysts, since proximity between the cyst membrane and mitochondria only occurred in specific positions (Fig. 3I). Meanwhile, the shortest distance measured between the mitochondria and the mature cyst wall was 37·8 nm, showing that cyst membranes were not closely associated with mitochondria (Fig. 3J). In conclusion, our data show that the intimate association of host cell mitochondria with the PVM is not maintained as PVs convert into cysts.

Lysosomes (but not early or late endosomes) accumulate around the cyst wall

To examine if the reorganization of microtubules around the cyst allows the recruitment of endosomes and lysosomes to the cyst

https://doi.org/10.1017/S0031182017002050 Published online by Cambridge University Press

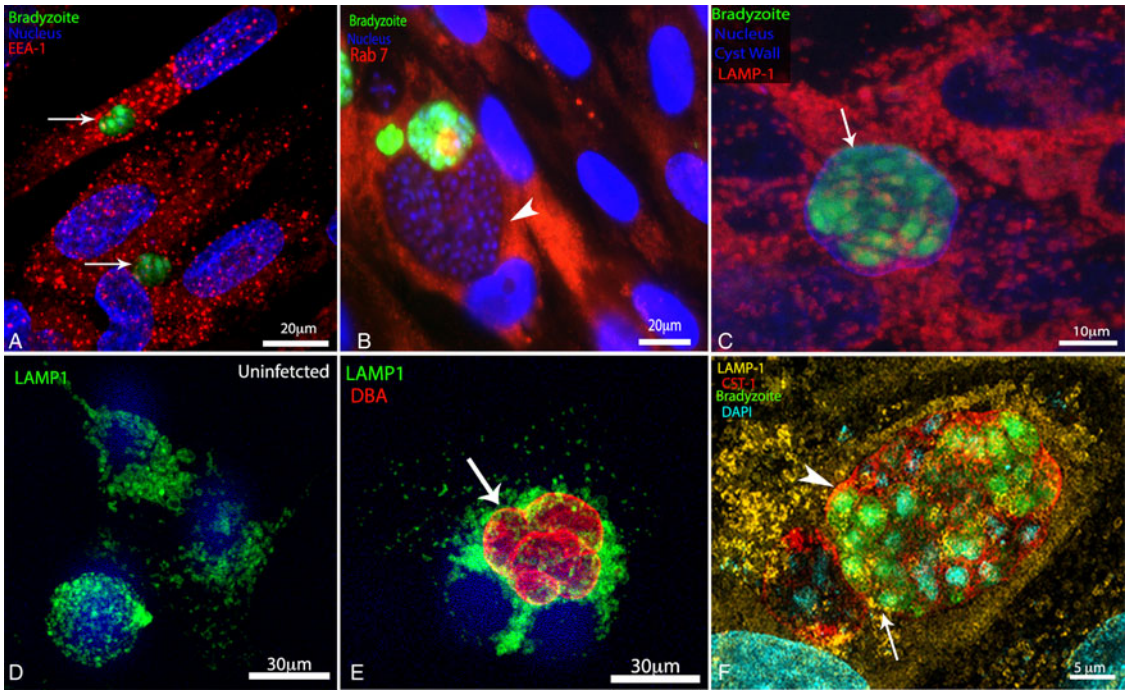

Fig. 4. Organization of the endolysosomal system during infection with *Toxoplasma gondii* cysts. LLC-MK_2 and human foreskin fibroblasts (HFF) cells were subjected to chronic infection with wild-type EGS or with the Bgreen strain (which produces GFP-labelled bradyzoites) and then labelled with markers for the endolysosomal system. Wild-type cysts were identified by labelling of the cyst wall with *Dolichos biflorus agglutin* (DBA)-FITC, and the DNA was stained with Hoescht 33342. (A) Distribution of early endosomes (labelled with an anti-EEA1 antibody, in red) in HFF infected with bradyzoites (green), within cysts (arrows). (B) Distribution of late endosomes (labelled with an anti-Rab7 antibody, in red) in HFF infected with bradyzoites (green, arrow) and tachyzoites (arrowhead) simultaneously. (C) Distribution of lysosomes (labelled with an anti-LAMP1 antibody) in HFF cells infected with bradyzoites (in green, with lysosomes in red). (D, E) Uninfected (D) and bradyzoite-infected LLC-MK_2 cells (E). Lysosomes (in green) were located close to the cyst wall (in red, arrow). (F) Super-resolution structured illumination imaging (SR-SIM) of an infected HFF showing the lysosomes (labelled with an anti-LAMP1 antibody, in yellow) juxtaposed to the cyst wall (labelled with an anti-CST1 antibody, in red).

periphery, infected cells were labelled with markers for early and late endosomal compartments (EEA1 and Rab7, respectively), and lysosomes (LAMP-1). The labelling of early and late endosomes in uninfected and infected HFF showed no preferential localization of these structures around EGS cysts (Fig. 4A and B). However, lysosomes were conspicuously concentrated around the cyst wall in infected HFF (Fig. 4C, E and F), while uninfected cells had lysosomes distributed throughout the cytoplasm, and surrounding the nucleus (Fig. 4D).

SR-SIM of HFF infected with cysts confirmed the close association of host lysosomes with the cyst wall (Fig. 4F). Live cell imaging of cyst-containing cells labelled with Lysotracker® showed that lysosomes, which are dynamic organelles in uninfected cells, were strictly localized around the boundary of bradyzoite-containing vacuoles during the period of image acquisition (Supplementary Fig. S2).

The endocytic tracer horseradish peroxidase (HRP) internalized by host cells reaches bradyzoites, inside cysts

The accumulation of lysosomes (but not of early or late endosomes) around the cyst wall suggests that the endocytic pathway of infected cells is focused on cysts – with nutrients internalized by host cells traversing the endocytic pathway and reaching lysosomes that are ideally positioned for nutrient uptake by cysts. To verify if nutrients ingested by host cells accumulated in lysosomes around cysts, cells infected with bradyzoites were incubated with tracers for fluid-phase (BSA) and receptor-mediated (transferrin) endocytosis tagged with fluorescent markers, and then aliquots were fixed at 15-min intervals, for uptake monitoring by IFA. Lysosomes positive for BSA-Alexa594 were observed around vacuoles containing bradyzoites after 1 h of incubation with the fluorescent tracer (Fig. 5A). Vesicles positive for transferrin-Alexa594 also accumulated around bradyzoite-containing vacuoles, after 30 min of incubation with the endocytic tracer (Fig. 5B). We did not observe differences in the kinetics of either fluid-phase or receptor-mediated endocytosis between infected and uninfected cells.

Despite the accumulation of fluorescently-labelled BSA and transferrin around cysts, gold-labelled transferrin and BSA internalized by host cells were not observed inside bradyzoites, by TEM. However, TEM analysis of LLC-MK_2 cells infected with cysts and incubated with the fluid-phase endocytosis marker HRP showed a clear positive reaction for peroxidase in cytoplasmic compartments of bradyzoites (Fig. 5C), showing a correlation between host endocytosis/vesicle traffic and cyst formation. To examine this correlation in more detail, we treated infected cells with taxol and evaluated the uptake of HRP by parasites. We observed that in the group of infected cells treated with taxol the number of parasites containing HRP-positive vesicles decreased by 4-fold (Supplementary Fig. S3). TEM images also revealed that transferrin-Au reached the rhoptries of tachyzoites after 45 min of incubation of infected LLC-MK_2 cells with this endocytosis tracer (Fig 5D, arrow). Altogether, the results of endocytosis assays demonstrate that nutrients accumulated in lysosomes that are recruited to the cyst periphery are transferred from host cells to bradyzoites, but in a selective manner.

Discussion

The infection of host cells by the tachyzoite form of *Toxoplasma gondii* leads to a series of modifications in the host cell metabolism and organelle distribution (Sinai *et al.* 1997; Melo *et al.* 2001; Magno *et al.* 2005; Coppens *et al.* 2006; Walker *et al.* 2008; Wang *et al.* 2010; Romano *et al.* 2013; Pernas *et al.* 2014). These

https://doi.org/10.1017/S0031182017002050 Published online by Cambridge University Press

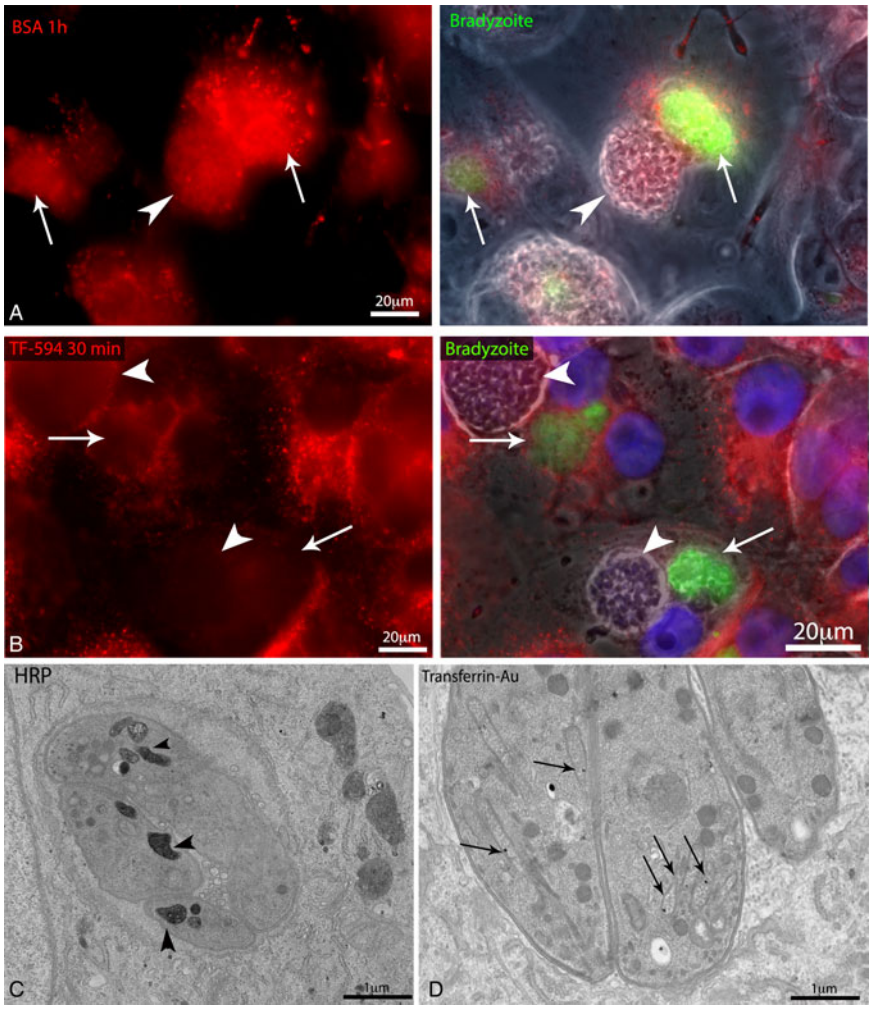

Fig. 5. Evaluation of the dynamic interaction between lysosomes and the *Toxoplasma gondii* cyst. Lysosome dynamics was evaluated by labelling/loading of lysosomes in LLC-MK_2 and human foreskin fibroblasts (HFF) cells infected with wild-type EGS or with the Bgreen strain (which produces GFP-labelled bradyzoites), followed by fluorescence and electron microscopy analyses. (A) LLC-MK_2 cells infected with Bgreen cysts (arrow) and parasitophorous vacuoles (PVs, arrowhead). The host cell lysosomes, which were preloaded with bovine serum albumin (BSA)-Alexa594 (by fluid phase endocytosis for 30 min), appear accumulated are around the cysts. (B) Fluorescence image of LLC-MK_2 cells infected with Bgreen cysts (arrows) and PVs (arrowheads). The lysosomes were loaded for 30 min before fixation with transferrin (Tf)-Alexa594 (by receptor-mediated endocytosis). Transferrin-positive lysosomes (in red) surrounded the cysts. (C, D) Transmission electron microscopy (TEM) of LLC-MK_2 infected with cysts and PVs and then loaded with endocytosis tracers (transferrin coupled to 10-nm colloidal gold (Tf-Au), and horseradish peroxidase, or HRP). (C) Tf-Au particles were found inside the rhoptries of tachyzoites (arrows). (D) Bradyzoites contained HRP-positive cytoplasmic compartments (arrowheads).

associations are not merely morphological and contribute to the intracellular survival of *T. gondii*, by granting the parasite access to host cell resources (Romano and Coppens, 2013; Coppens, 2014).

While the recruitment/diversion of host cell resources by tachyzoites had been well described, we show here that intracellular development of cysts containing bradyzoite forms, *in vitro*, also involves specific events of reorganization of the host cell cytoplasm that may facilitate cyst maintenance.

One of the first drastic changes coordinated by intracellular pathogens in the host cell architecture is the reorganization of cytoskeletal elements (Jimenez *et al.* 2016). The distribution of actin microfilaments was not altered during the conversion of *T. gondii* tachyzoites into bradyzoites (Fig. 1A and B), suggesting that these filaments do not play a key role in cystogenesis. Thus, *T. gondii* cysts differ from other intracellular pathogens, such as *Leishmania*, which rely on the anchoring of actin microfilament to the vicinity of the PV, to prevent the fusion of PVs with lysosomes, before the differentiation to a more resistant parasite stage (Moradin and Descoteaux, 2012). Also, intracellular bacteria such as *Rickettsia* spp., *Chlamydia* sp. and *Legionella* spp. use the host cell actin microfilament network to invade, establish the PV and escape from the host cell (Colonne *et al.* 2016).

The tachyzoite-containing PV is positioned near the nuclear region right after invasion, and recruits to its vicinity the host cell centrosome (Melo *et al.* 2001; Walker *et al.* 2008; Wang *et al.* 2010; Cardoso *et al.* 2016), which is likely to divert vesicular traffic towards the PV. In contrast to the lack of microfilament reorganization during cystogenesis, we show here that the cage-like organization of microtubules around the PV persists during cyst formation, with microtubules seen orderly positioned around the cyst and closely associated with the cyst wall membrane.

The role of microtubules in the acquisition of cholesterol-derived LDL by *T. gondii* tachyzoites is well described (Coppens *et al.* 2006) and, interestingly, starvation of LDL induced stage conversion to bradyzoites in infected CHO cells (Ihara and Nishikawa, 2014). Under starving or low nutrient conditions, tachyzoites convert to bradyzoites, as a strategy to survive and persist under harsh conditions (Sullivan and Jeffers, 2012). Thus, the increased encystation rates observed here after treatment with the microtubule stabilizer taxol could be explained by a reduction in nutrient supply to PVs in the absence of microtubule dynamics, which supports the notion that a dynamic microtubule network is necessary to mobilize nutritional resources from host cell organelles to PVs.

Cystogenesis also resulted in the reorganization of the host cell intermediate filament network. As previously described for PVs (Halonen and Weidner, 1994; Halonen *et al.* 1998), bundles of intermediate filaments were seen around the cysts. These bundles most likely confer resistance and mechanical protection to the cyst, as they do to the PV (Halonen and Weidner, 1994; Halonen *et al.* 1998). Our data demonstrated that the accumulation of host cell intermediate filaments is more pronounced around cysts than around PVs, suggesting that more filaments are added to the periphery of the cyst, during cystogenesis. Overall, we showed that the cyst attracts microtubules and intermediate filaments to its vicinity, and that these cytoskeletal structures form a 'cage' that is likely to provide mechanical protection for life-long cyst maintenance in the intracellular environment.

https://doi.org/10.1017/S0031182017002050 Published online by Cambridge University Press

The concentration of microtubules around cysts could have the double role of providing mechanical support to the growing cyst and facilitating the movement of organelles from the endo and exocytic host pathways towards the cyst, favouring nutrient scavenging by bradyzoites. Although we observed occasional relocation of the Golgi complex to the vicinity of the cysts, the Golgi was not consistently positioned close to the cyst. Treatment with brefeldin A (which disrupts anterograde traffic to the Golgi) had no significant effect on the rate of spontaneous cysts formation. In conclusion, cystogenesis does not seem to require proximity or interaction with the Golgi complex. In contrast, proximity to the Golgi complex and the presence of Golgi-derived vesicles inside the PV are essential for the complete development of the tachyzoite form, which scavenges sphingolipids *via* Golgi association (in type I and type II *T. gondii* strains) (Romano *et al.* 2013). This lack of requirement for proximity to the Golgi complex indicates that, metabolically, bradyzoites do not depend on Golgi-derived sphingolipids for their maintenance, which will require further investigation.

The association and docking of endoplasmic reticulum lamellae around the PVM described for the acute stage (Sinai *et al.* 1997; Magno *et al.* 2005) was also observed here during cystogenesis, and in the established bradyzoite stage, with endoplasmic reticulum lamellae consistently observed within folds of the cyst membrane. Nevertheless, when infected host cells were treated with tunicamycin, which impairs N-glycosylation in the ER, the spontaneous formation of cysts was not affected. Our results contrast with those obtained by Narasimhan *et al.* (2008), who reported that stress induced by treatment with tunicamycin triggers cyst formation in HFF cell infected with the type II strain ME-49 (Narasimhan *et al.* 2008). In our analysis, tunicamycin treatment had no effect on the rate of cystogenesis *in vitro*, even though our TEM data show a clear association of ER profiles with the wrinkled cyst membrane. Furthermore, numerous ER-derived vesicles were seen juxtaposed to the cyst wall membrane, both by SR-SIM and by electron microscopy tomography. The proximity between ER and cyst membranes suggests that the ER could donate membranes to allow cyst growth, or that ER-derived molecules may be delivered to the interior of cysts. The relationship between PV-enclosed pathogens and the host ER is widely explored in bacterial infection (Truchan *et al.* 2016), where bacteria such as *Legionella* sp, *Brucella* sp. and *Chlamydia* sp. fuse to ER sites and trigger the unfolded protein response (UPR), which facilitates infection development, and also use the ER as a replication niche (Celli and Tsolis, 2015). Thus, maintenance of ER association, during PV-to-cyst conversion, could be essential to perpetuate chronic infection.

Host cell mitochondria associate with intracellular pathogens to allow the nutrient transfer, and also to trigger infected cell apoptosis, as part of innate immunity (Pernas *et al.* 2014). During tachyzoite infection, mitochondria are physically associated with the PV, and in type I and III strains of *T. gondii* this association is mediated by the protein MAF-1 (Sinai *et al.* 1997; Pernas and Boothroyd, 2010; Pernas *et al.* 2014). This protein is not expressed in type II strains, where the mitochondria do not appear associated with PVs (Pernas *et al.* 2014). Our results show that, during infection with the natural hybrid (mixed type I and type III) strain EGS, mitochondria appear concentrated around the PV membrane, but not around the cyst wall, even in cells bearing PVs (containing tachyzoites) and cysts simultaneously. Analyses of the mRNA expression profiles of the EGS hybrid strain (McPhillie *et al.* 2016) did not show alteration on the expression levels of MAF-1 during tachyzoite to bradyzoites conversion. However, our TEM images clearly suggest that EGS cysts formed *in vitro* were not closely associated with host mitochondria; thus, the mitochondrial association does not appear essential for bradyzoite infection.

We also investigated the reorganization of the endolysosomal system in cells with *T. gondii* cysts. Early and late endosomes were not preferentially located around the cyst wall membrane, while the lysosomes were closely associated with (and reorganized around) the cysts boundary, in infected cells. With the exception of the HRP tracer – which reached bradyzoites within 60 min of administration to infected host cells – none of the other classic endocytosis cargo (the fluid-phase tracer BSA and the receptor-mediated tracer transferrin) were observed to be scavenged by the cyst. However, intrinsic differences in the sensitivities of enzymatic activity and stochastic variation in gold-labelled tracer detection (in the absence of amplification) cannot be ruled out in TEM thin sections. In the tachyzoite stage, the PV sequesters lysosome-derived vesicles to capture cholesterol internalized by endocytosis (Coppens *et al.* 2006). In agreement with these data, we show here that transferrin internalized by host cells reaches the rhoptries of tachyzoites, inside PVs, but not the encysted bradyzoites. Overall, our data show that host cell lysosomes, although very close to the cyst membrane, did not transfer part of their endocytic content to cysts, indicating that the scavenging of nutrients by cysts, *via* the association with lysosomes, is somehow selective for certain cargos.

In conclusion, we observed that the distribution of host cell organelles around the PV is partially maintained during the chronic stage of *Toxoplasma* infection. Microtubules and intermediate filaments (but not microfilaments) are likely to provide mechanical support to the cyst, and endoplasmic reticulum lamellae were closely associated with the cyst wall membrane, while mitochondria were somewhat distant from the cyst wall (compared with their location relative to the PVM). Paradoxically, the close association of cysts with host cell lysosomes was not matched by effective transfer of internalized endocytic tracers to the cyst. The data presented in this work suggest specific differences in the way PVs and cysts utilize host cell resources. Future studies on the molecular machineries involved in the interface between the cyst wall and host organelles/structures may identify interesting targets for chemotherapeutic intervention on the chronic stage of toxoplasmosis.

Supplementary Material. The supplementary material for this article can be found at https://doi.org/10.1017/S0031182017002050

Acknowledgements. The authors thank Brunno Verçoza and Fernando Almeida – from Numpex Bio (UFRJ, Xerem, RJ, Brazil) and CENABIO (UFRJ, Rio de Janeiro, RJ, Brazil) for their expert technical assistance with advanced light microscopy imaging. The authors thank to Words in Science for the professional revision of the text.

Financial Support. This work was supported by CAPES, CNPq, FAPERJ.

References

Andrade EF, Stumbo AC, Monteiro-Leal LH, Carvalho L and Barbosa HS (2001) Do microtubules around the *Toxoplasma gondii*-containing parasitophorous vacuole in skeletal muscle cells form a barrier for the phagolysosomal fusion? *Journal of Submicroscopic Cytology and Pathology* **33**(3), 337–341.

Bereiter-Hahn J and Vöth M (1994) Dynamics of mitochondria in living cells: shape changes, dislocations, fusion, and fission of mitochondria. *Microscopy Research and Technique* **27**(3), 198–219.

Blader IJ, Coleman BI, Chen C-T and Gubbels M-J (2015) Lytic cycle of *Toxoplasma gondii*: 15 years later. *Annual Review of Microbiology* **69**(1), 150902154308007.

Cardoso R, Soares H, Hemphill A and Leitão A (2016) Apicomplexans pulling the strings: manipulation of the host cell cytoskeleton dynamics. *Parasitology* 1–14.

Celli J and Tsolis RM (2015) Bacteria, the endoplasmic reticulum and the unfolded protein response: friends or foes? *Nature Reviews. Microbiology* **13**(2), 71–82.

Colonne PM, Winchell CG and Voth DE (2016) Hijacking host cell highways: manipulation of the host actin cytoskeleton by obligate intracellular bacterial pathogens. *Frontiers in Cellular and Infection Microbiology* **6**, 107.

Coppens I (2014) Exploitation of auxotrophies and metabolic defects in Toxoplasma as therapeutic approaches. *International Journal for Parasitology* **44**(2), 109–120.

Coppens I, Dunn JD, Romano JD, Pypaert M, Zhang H, Boothroyd JC and Joiner KA (2006) *Toxoplasma gondii* sequesters lysosomes from mammalian hosts in the vacuolar space. *Cell* **125**(2), 261–274.

de Souza W and Attias M (2015) New views of the *Toxoplasma gondii* parasitophorous vacuole as revealed by Helium Ion Microscopy (HIM). *Journal of Structural Biology* **191**(1), 76–85.

Dou Z, Mcgovern OL, Di Cristina M, Cristina D and Carruthers B (2014) *Toxoplasma gondii* ingests and digests host cytosolic proteins. *MBio* **5**(4), e01188-14.

Dubey JP, Lindsay DS and Speer CA (1998) Structures of *Toxoplasma gondii* tachyzoites, bradyzoites, and sporozoites and biology and development of tissue cysts. *Clinical Microbiology Reviews* **11**(2), 267–299.

Dzierszinski F, Nishi M, Ouko L and Roos DS (2004) Dynamics of *Toxoplasma gondii* differentiation. *Eukaryotic Cell* **3**(4), 992–1003.

Ferguson DJ and Hutchison WM (1987) An ultrastructural study of the early development and tissue cyst formation of *Toxoplasma gondii* in the brains of mice. *Parasitology Research* **73**(6), 483–491.

Ferreira ADM, Vitor RWA, Gazzinelli RT and Melo MN (2006) Genetic analysis of natural recombinant Brazilian *Toxoplasma gondii* strains by multilocus PCR-RFLP. *Infection, Genetics and Evolution: Journal of Molecular Epidemiology and Evolutionary Genetics in Infectious Diseases* **6**(1), 22–31.

Freyre A (1995) Separation of toxoplasma cysts from brain tissue and liberation of viable bradyzoites. *The Journal of Parasitology* **81**(6), 1008–1010.

Gold DA, Kaplan AD, Lis A, Bett GCL, Rosowski EE, Cirelli KM, Hakimi M, Rasmusson RL and Saeij JPJ (2015) The toxoplasma dense granule proteins GRA17 and GRA23 mediate the movement of small molecules between the host and the parasitophorous vacuole. *Cell Host & Microbe* **17**(5), 642–652.

Guimarães EV, Acquarone M, de Carvalho L and Barbosa HS (2007) Anionic sites on *Toxoplasma gondii* tissue cyst wall: expression, uptake and characterization. *Micron (Oxford, England: 1993)* **38**(6), 651–658.

Halonen SK and Weidner E (1994) Overcoating of Toxoplasma parasitophorous vacuoles with host cell vimentin type intermediate filaments. *The Journal of Eukaryotic Microbiology* **41**(1), 65–71.

Halonen SK, Weiss LM and Chiu FC (1998) Association of host cell intermediate filaments with *Toxoplasma gondii* cysts in murine astrocytes in vitro. *International Journal for Parasitology* **28**(5), 815–823.

Ihara F and Nishikawa Y (2014) Starvation of low-density lipoprotein-derived cholesterol induces bradyzoite conversion in *Toxoplasma gondii*. *Parasites & Vectors* **7**(1), 248.

Jimenez A, Chen D and Alto NM (2016) How bacteria subvert animal cell structure and function. *Annual Review of Cell and Developmental Biology* **32**(1), annurev-cellbio-100814-125227.

Kremer JR, Mastronarde DN, McIntosh JR (1995) Computer visualization of three-dimensional image data using IMOD. *Journal of structural biology* **116**, 71–76.

Lemgruber L, Lupetti P, Martins-Duarte ES, De Souza W and Vommaro RC (2011) The organization of the wall filaments and characterization of the matrix structures of *Toxoplasma gondii* cyst form. *Cellular Microbiology* **13**(12), 1920–1932.

Magno RC, Straker LC, de Souza W and Attias M (2005) Interrelations between the parasitophorous vacuole of *Toxoplasma gondii* and host cell organelles. *Microscopy and Microanalysis* **11**(2), 166–174.

McPhillie M, Zhou Y, El Bissati K, Dubey J, Lorenzi H, Capper M, Lukens AK, Hickman M, Muench S, Verma SK, Weber CR, Wheeler K, Gordon J, Sanders J, Moulton H, Wang K, Kim T-K, He Y, Santos T, Woods S, Lee P, Donkin D, Kim E, Fraczek L, Lykins J, Esaa F, Alibana-Clouser F, Dovgin S, Weiss L, Brasseur G, Wirth D, Kent M, Hood L, Meunieur B, Roberts CW, Hasnain SS, Antonyuk SV, Fishwick C and McLeod R (2016) New paradigms for understanding and step changes in treating active and chronic, persistent apicomplexan infections. *Scientific Reports* **6**, 29179.

Melo EJ, Carvalho TM and De Souza W (2001) Behaviour of microtubules in cells infected with *Toxoplasma gondii*. *Biocell* **25**(1), 53–59.

Montoya JG and Liesenfeld O (2004) Toxoplasmosis. *Lancet* **363**(9425), 1965–1976.

Moradin N and Descoteaux A (2012) Leishmania promastigotes: building a safe niche within macrophages. *Frontiers in Cellular and Infection Microbiology* **2**, 121.

Narasimhan J, Joyce BR, Naguleswaran A, Smith AT, Livingston MR, Dixon SE, Coppens I, Wek RC and Sullivan WJ (2008) Translation regulation by eukaryotic initiation factor-2 kinases in the development of latent cysts in *Toxoplasma gondii*. *Journal of Biological Chemistry* **283**(24), 16591–16601.

Paredes-Santos TC, Martins-Duarte ES, Vitor RWA, de Souza W, Attias M and Vommaro RC (2013) Spontaneous cystogenesis in vitro of a Brazilian strain of *Toxoplasma gondii*. *Parasitology International* **62**(2), 181–188.

Paredes-Santos TC, Tomita T, Yan Fen M, de Souza W, Attias M, Vommaro RC and Weiss LM (2016) Development of dual fluorescent stage specific reporter strain of *Toxoplasma gondii* to follow tachyzoite and bradyzoite development in vitro and in vivo. *Microbes and Infection* **18**(1), 39–47.

Pernas L and Boothroyd JC (2010) Association of host mitochondria with the parasitophorous vacuole during Toxoplasma infection is not dependent on rhoptry proteins ROP2/8. *International Journal for Parasitology* **40**(12), 1367–1371.

Pernas L, Adomako-Ankomah Y, Shastri AJ, Ewald SE, Treeck M, Boyle JP and Boothroyd JC (2014) Toxoplasma effector MAF1 mediates recruitment of host mitochondria and impacts the host response. *PLoS Biology* **12**(4), e1001845.

Popiel I, Gold MC and Booth KS (1996) Quantification of *Toxoplasma gondii* bradyzoites. *The Journal of Parasitology* **82**(2), 330–332.

Romano JD and Coppens I (2013) Host Organelle Hijackers: a similar modus operandi for *Toxoplasma gondii* and *Chlamydia trachomatis*: co-infection model as a tool to investigate pathogenesis. *Pathogens and Disease* **69**(2), 72–86.

Romano JD, Sonda S, Bergbower E, Smith ME and Coppens I (2013) *Toxoplasma gondii* salvages sphingolipids from the host Golgi through the rerouting of selected Rab vesicles to the parasitophorous vacuole. *Molecular Biology of the Cell* **24**(12), 1974–1995.

Schwab JC, Beckers CJ and Joiner KA (1994) The parasitophorous vacuole membrane surrounding intracellular *Toxoplasma gondii* functions as a molecular sieve. *Proceedings of the National Academy of Sciences of the United States of America* **91**(2), 509–513.

Sheffield HG and Melton ML (1968) The fine structure and reproduction of *Toxoplasma gondii*. *The Journal of Parasitology* **54**(2), 209–226.

Sinai AP, Webster P and Joiner KA (1997) Association of host cell endoplasmic reticulum and mitochondria with the *Toxoplasma gondii* parasitophorous vacuole membrane: a high affinity interaction. *Journal of Cell Science* **110**(Pt 1), 2117–2128.

Sullivan WJ and Jeffers V (2012) Mechanisms of *Toxoplasma gondii* persistence and latency. *FEMS Microbiology Reviews* **36**(3), 717–733.

Suzuki Y, Orellana MA, Schreiber RD and Remington JS (1988) Interferon-gamma: the major mediator of resistance against *Toxoplasma gondii*. *Science (New York, N.Y.)* **240**(4851), 516–518.

Sweeney KR, Morrissette NS, LaChapelle S and Blader IJ (2010) Host cell invasion by *Toxoplasma gondii* is temporally regulated by the host microtubule cytoskeleton. *Eukaryotic Cell* **9**(11), 1680–1689.

Tomita T, Bzik DJ, Ma YF, Fox BA, Markillie LM, Taylor RC, Kim K and Weiss LM (2013) The *Toxoplasma gondii* cyst wall protein CST1 is critical for cyst wall integrity and promotes bradyzoite persistence. *PLoS Pathogens* **9**(12), e1003823.

Truchan HK, Cockburn CL, Hebert KS, Magunda F, Noh SM and Carlyon JA (2016) The pathogen-occupied vacuoles of anaplasma phagocytophilum and anaplasma marginale interact with the endoplasmic reticulum. *Frontiers in Cellular and Infection Microbiology* **6**, 22.

Vieira P, Vidigal T, Vítor D, Santos V, Castro FC and César J (2002) Prenatal toxoplasmosis diagnosis from amniotic fluid by PCR. *Revista Da Sociedade Brasileira de Medicina Tropical* **35**(1), 1–6.

Walker ME, Hjort EE, Smith SS, Tripathi A, Hornick JE, Hinchcliffe EH, Archer W and Hager KM (2008) *Toxoplasma gondii* actively remodels the microtubule network in host cells. *Microbes and Infection* **10**(14–15), 1440–1449.

Wang Y, Weiss LM and Orlofsky A (2010) Coordinate control of host centrosome position, organelle distribution, and migratory response by *Toxoplasma gondii via* host mTORC2. *Journal of Biological Chemistry* **285**(20), 15611–15618.

https://doi.org/10.1017/S0031182017002050 Published online by Cambridge University Press

Watts E, Zhao Y, Dhara A, Eller B, Patwardhan A & Sinai P (2015) Novel approaches reveal that *Toxoplasma gondii* bradyzoites within tissue cysts are dynamic and replicating entities in vivo. *MBio* **6**(5), 1–24.

Weiss LM and Kim K (2000) The development and biology of bradyzoites of *Toxoplasma gondii*. *Frontiers in Bioscience: A Journal and Virtual Library* **5**, D391–D405.

White MW, Radke JR and Radke JB (2014) Microreview Toxoplasma development – turn the switch on or off? *Cellular Microbiology* **16**, 466–472.

Zhang YW, Halonen SK, Ma Y, Wittner M, Weiss LM and Mmun INI (2001) Initial characterization of CST1, a *Toxoplasma gondii* cyst wall glycoprotein. *Infection and Immunity* **69**(1), 501–507.

https://doi.org/10.1017/S0031182017002050 Published online by Cambridge University Press